

Study of Structural and Electrical Transport Properties of Sn Doped $\text{La}_2\text{Mn}_2\text{O}_7$

SHAHID HUSAIN*, M. WASI KHAN

Department of Physics, Aligarh Muslim University, Aligarh-202002, India

The character of charge carriers in the manganites can be changed to n-type by replacing La^{3+} with tetravalent ions like Ce, Sn, Zr etc. A combination of n- and p-type oxides can form a p-n junction that can be used as a functional device for various applications. Therefore, the recently developed n-type La-Sn-Mn-O compound has attracted much research interest. We have synthesized the $(\text{La}_{1-x}\text{Sn}_x)_2\text{Mn}_2\text{O}_7$ ($x = 0.1, 0.2$ and 0.3) in bulk form using solid state reaction route. These samples were characterized using x-ray diffraction and temperature dependence resistivity measurements. Rietveld analysis is performed using the FULLPROF code to ensure the single phase nature of the samples. PowderX technique is used for peak indexing and to determine the lattice parameters. The variation in lattice parameters has been observed and the unit cell volume increases with the increase in Sn concentration. The metal-insulator transition is observed for all the samples. We have fitted our resistivity data for the different temperature ranges, with the help of theoretical models. At low temperatures below transition temperature (T_c), the data fits well with the expression: $\rho = \rho_0 + \rho_1 T^{2.5}$. This suggests that electron-electron, electron-phonon, and electron-magnon interactions are responsible for variation in resistivity below T_c . The higher temperature data follows the relation: $\rho(T) = \rho_0 T \exp(E_a/k_B T)$. This shows that the conductivity above the transition temperature is due to small polaron hopping.

(Received April 1, 2008; accepted June 30, 2008)

Keywords: Manganites, Metal-insulator transition, Small polaron hopping

1. Introduction

Since the end of last century, the colossal magnetoresistance (CMR) phenomenon in perovskite manganites has become an important research subject for its potential applications. The metal-insulator transition and magnetic transition are also observed in these systems. These phenomena are traditionally explained on the basis of double exchange model and Jahn-Teller distortion effects. Generally, the manganese ions in LaMnO_3 exist in 3^+ valence state, when a divalent ion such as Ca, Sr, Ba etc. is substituted for a part of La, proportionate amount of Mn^{3+} ions convert into Mn^{4+} ions. This type of compounds show hole conductivity. On the other hand, when a tetravalent ion is substituted in place of La, proportionate amount of Mn^{3+} ions convert into Mn^{2+} ions and resultant manganite is termed as electron doped manganite. But it is very difficult to obtain single phase electron doped manganites due to large size differences between trivalent La and tetravalent ions.

Mandal and Das [1] initiated the work on electron doped manganites by doping Ce in LaMnO_3 . Their structural and transport analysis showed signatures of mixed phases and hence blurred the interpretation of the obtained results. Later on, some reports appeared [2,3] in which it was suggested that Ce doped LaMnO_3 can be synthesized in thin film form but not in bulk form. In view of abovementioned reports, we have prepared the Ce doped LaMnO_3 in bulk as well as in thin film form and measured their structural, electrical and magneto-transport properties [4,5]. Our samples in bulk and thin film form have not displayed any double transition in temperature dependence of resistivity measurements as reported

previously. This study encouraged us to synthesized other electron doped manganites like Sn doped LaMnO_3 . As compared to Ce, Sn doping at La site encounters an even more severe challenge due to the larger ionic size misfit between La^{3+} and Sn^{4+} .

CMR effect has been reported in several systems like $\text{La}_{1-x}\text{Sn}_x\text{MnO}_3$ and Fe doped $\text{La}_{1-x}\text{Sn}_x\text{MnO}_3$ [6-8]. These reports indicate that $\text{La}_{1-x}\text{Sn}_x\text{MnO}_3$ does not form in single phase. But it is a mixture of LaMnO_3 and $\text{La}_2\text{Mn}_2\text{O}_7$ phases. In consideration of these reports we have undertook the synthesis of $(\text{La}_{1-x}\text{Sn}_x)_2\text{Mn}_2\text{O}_7$ ($x = 0.1, 0.2$ and 0.3) and studied their structural and electrical transport properties.

2. Experimental

We have prepared the samples of $(\text{La}_{1-x}\text{Sn}_x)_2\text{Mn}_2\text{O}_7$ ($x = 0.1, 0.2$ and 0.3) by the solid state reaction method. The stoichiometric amounts of La_2O_3 , SnO_2 and MnO_2 (All of AR grade) in powdered form were ground in an agate mortar till a homogeneous mixture is formed. This mixture was kept in an alumina boat and heated at $1000\text{ }^\circ\text{C}$ for 24 hours. This preheated powder was again ground and heated at $1100\text{ }^\circ\text{C}$ in air for 72 hours with intermediate grindings. Finally, reacted powder was pressed in the form of pellets and heated at $1100\text{ }^\circ\text{C}$ in air for 24 hours and then furnace cooled to room temperature. The powder x-ray diffraction patterns were recorded using Bruker D8 x-ray diffractometer. The electrical resistivity as a function of temperature was performed using four probe technique in the temperature range 77-300 K.

3. Results and discussion

3.1 Structural Analysis

We have performed the powder x-ray diffraction measurement at room temperature and fitted the x-ray diffraction patterns using FULLPROF code for Rietveld analysis of these samples. The diffraction patterns for $(La_{1-x}Sn_x)_2Mn_2O_7$ ($x = 0.1, 0.2$ and 0.3) have been shown in Fig 1. The analysis for these patterns reveals that all the samples are formed in the double layered structure with orthorhombic crystal symmetry having space group Pnma. The lattice parameters and unit cell volume of $La_2Mn_2O_7$ alter considerably with the change in Sn concentration. These variations in lattice parameters and unit cell volume have been summarized in Table 1 and shown in Fig.2. The increase in unit cell volume is obvious as Sn has larger atomic radius as compared to La.

Table 1. The lattice parameters and the unit cell volume of $(La_{1-x}Sn_x)_2Mn_2O_7$ ($x = 0.1, 0.2$ and 0.3).

| Composition | Crystal Symmetry | a (Å) | b (Å) | c (Å) | Unit cell volume (Å ³) |
|-------------------------------|------------------|---------|---------|---------|------------------------------------|
| $(La_{0.9}Sn_{0.1})_2Mn_2O_7$ | Orthorhombic | 8.65 | 7.44 | 8.97 | 577.27 |
| $(La_{0.8}Sn_{0.2})_2Mn_2O_7$ | Orthorhombic | 8.65 | 7.46 | 8.97 | 578.92 |
| $(La_{0.7}Sn_{0.3})_2Mn_2O_7$ | Orthorhombic | 9.12 | 9.56 | 9.77 | 852.17 |

We have calculated all the lattice parameters with the help of PowderX software. The maximum deviation that occurred between the observed and calculated values of interplanar spacing (d value) remains below 0.01 Å, barring a few d -values where deviation exceeds from this value but remains under 0.05 Å. But in most of the cases there is hardly any difference between the two values.

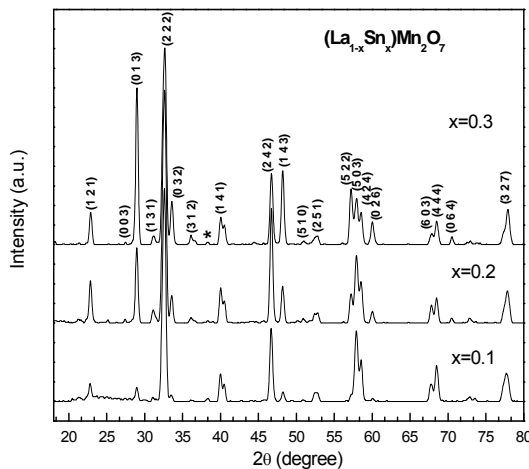


Fig. 1 Powder x-ray diffraction patterns of $(La_{1-x}Sn_x)_2Mn_2O_7$ ($x = 0.1, 0.2$ and 0.3).

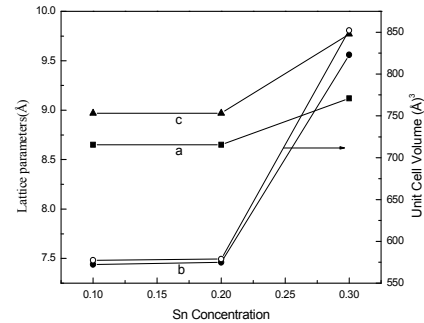


Fig. 2 The variation of lattice parameters and unit cell volume with Sn concentration.

3.2 Transport Analysis

We have measured the resistivity of $(La_{1-x}Sn_x)_2Mn_2O_7$ ($x = 0.1, 0.2$ and 0.3) as a function of temperature. All the samples exhibit metal insulator transition (MIT) as shown in Fig.3. The transition temperatures (T_c) are tabulated in Table 1. This phenomenon is traditionally explained by double exchange model [9] and Jahn-Teller effect [10]. As the temperature increases more and more Mn^{4+} ions take up the antiparallel spin orientations and the e_g electrons of the Mn^{3+} with parallel spins encounter more resistance until at T_c , when the spin polarization completes and the resistance becomes maximum. The system stays in this condition for some range of temperatures after which thermal excitation of electron starts and semiconductor action becomes operative.

In the semiconducting region ($T > T_c$), the temperature dependence of resistivity can be best fitted with the expression:

$$\rho(T) = \rho_0 T \exp(E_a/k_B T)$$

where k_B is the Boltzmann constant, ρ_0 is the resistivity coefficient and E_a is the activation energy. These fits have been shown in Fig.4. We can see the linear curves confirming the fit and the fitted data are shown as solid lines. The expression is based on the conduction model of small polaron hopping [11]. In the manganites systems at high temperature the lattice becomes distorted around the electrons in the conduction band and due to the strong electron-phonon interaction, small polarons are formed.

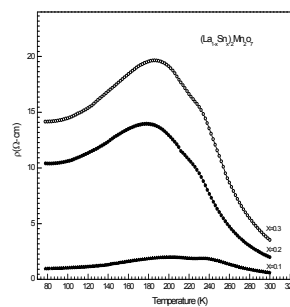


Fig. 3. Temperature dependence of resistivity plots for $(La_{1-x}Sn_x)_2Mn_2O_7$ ($x = 0.1, 0.2$ and 0.3).

Table 1. The transition temperature for different compositions of $(\text{La}_{1-x}\text{Sn}_x)_2\text{Mn}_2\text{O}_7$ ($x = 0.1, 0.2, 0.3$).

| S.No. | Composition | Transition temperature T_c |
|-------|---|------------------------------|
| 1 | $(\text{La}_{0.9}\text{Sn}_{0.1})_2\text{Mn}_2\text{O}_7$ | 200K |
| 2 | $(\text{La}_{0.8}\text{Sn}_{0.2})_2\text{Mn}_2\text{O}_7$ | 178K |
| 3 | $(\text{La}_{0.7}\text{Sn}_{0.3})_2\text{Mn}_2\text{O}_7$ | 186K |

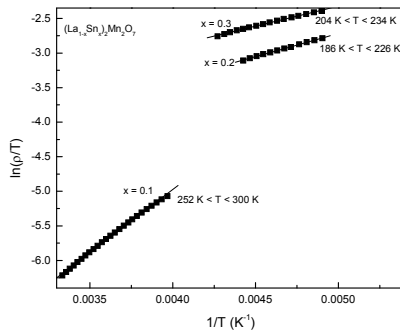


Fig. 4. $\ln(\rho/T)$ versus $1/T$ plots for different compositions of $(\text{La}_{1-x}\text{Sn}_x)_2\text{Mn}_2\text{O}_7$ above T_c .

The thermally activated hopping of these polarons plays an important role in this state. The activation energy, E_a , calculated using these fits is tabulated in Table 2. The activation energy is found to be increase with the increase in the Sn concentration.

Table 2. Activation energy E_a for different compositions of $(\text{La}_{1-x}\text{Sn}_x)_2\text{Mn}_2\text{O}_7$ ($x = 0.1, 0.2, 0.3$).

| Compositions | E_a (meV) |
|---|-----------------------|
| $(\text{La}_{0.9}\text{Sn}_{0.1})_2\text{Mn}_2\text{O}_7$ | 157.2955 ± 1.3895 |
| $(\text{La}_{0.8}\text{Sn}_{0.2})_2\text{Mn}_2\text{O}_7$ | 157.6025 ± 1.3938 |
| $(\text{La}_{0.7}\text{Sn}_{0.3})_2\text{Mn}_2\text{O}_7$ | 161.2036 ± 1.8774 |

Table 3. The values of ρ_1 and ρ_2 for different compositions of $(\text{La}_{1-x}\text{Sn}_x)_2\text{Mn}_2\text{O}_7$ ($x = 0.1, 0.2, 0.3$).

| Composition | ρ_1 ($\Omega\text{-cm}$) | ρ_2 ($\Omega\text{-cm-K}^{-2}$) |
|---|---------------------------------|---|
| $(\text{La}_{0.9}\text{Sn}_{0.1})_2\text{Mn}_2\text{O}_7$ | 0.808 ± 0.00388 | $2.3208 \times 10^{-5} \pm 3.52 \times 10^{-7}$ |
| $(\text{La}_{0.8}\text{Sn}_{0.2})_2\text{Mn}_2\text{O}_7$ | 8.6004 ± 0.03169 | $1.9269 \times 10^{-4} \pm 1.8278 \times 10^{-6}$ |
| $(\text{La}_{0.7}\text{Sn}_{0.3})_2\text{Mn}_2\text{O}_7$ | 11.56655 ± 0.03769 | $2.6887 \times 10^{-4} \pm 1.949 \times 10^{-6}$ |

We have also fitted the data in the same temperature range using the relation

$$\rho = \rho_0 + \rho_1 T^{2.5}$$

where ρ_0 is the resistivity due to domain boundaries and other temperature independent scattering mechanism and $\rho_1 T^{2.5}$ term is an empirical fit to the data which represents a combination of electron-electron, electron-phonon and electron-magnon scattering [12]. These plots have been shown in Fig.6. The values of ρ_0 and ρ_1 calculated from these fits are tabulated in Table4.

In the metallic state ($T < T_c$) the data is fitted with the following expression:

$$\rho = \rho_1 + \rho_2 T^n$$

with $n = 2$. ρ_1 and ρ_2 are constants. The ρ versus T^2 graphs have been plotted as shown in Fig.5.

The values of ρ_1 and ρ_2 calculated using these plots are tabulated in Table 3. It is well known that T^2 dependence is due to electron-electron scattering according to Fermi liquid model. This fit shows that the double exchange interaction plays an important role in case of Sn doped manganites. $\rho_2 T^2$ term indicates the resistivity due to electron-electron scattering process.

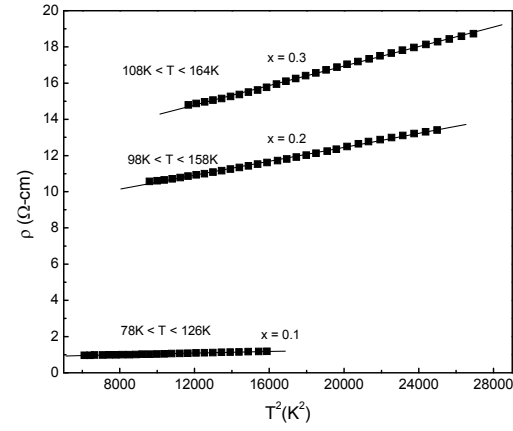


Fig. 5. Resistivity versus T^2 plots for $(\text{La}_{1-x}\text{Sn}_x)_2\text{Mn}_2\text{O}_7$ ($x = 0.1, 0.2, 0.3$).

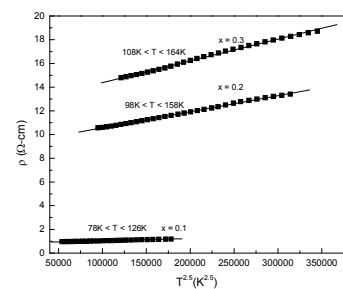


Fig. 6. Resistivity versus $T^{2.5}$ plots for $(\text{La}_{1-x}\text{Sn}_x)_2\text{Mn}_2\text{O}_7$ ($x = 0.1, 0.2$ and 0.3).

Table 4. The values of ρ_0 and ρ_1 for different compositions of $(La_{1-x}Sn_x)_2Mn_2O_7$ ($x = 0.1, 0.2, 0.3$).

| Composition | ρ_0 ($\Omega\text{-cm}$) | ρ_1 ($\Omega\text{-cm-K}^{-2.5}$) |
|-------------------------------|---------------------------------|---|
| $(La_{0.9}Sn_{0.1})_2Mn_2O_7$ | 0.85505 ± 0.00206 | $1.8279 \times 10^{-6} \pm 1.7860 \times 10^{-8}$ |
| $(La_{0.8}Sn_{0.2})_2Mn_2O_7$ | 9.21682 ± 0.01707 | $1.3541 \times 10^{-5} \pm 8.3994 \times 10^{-8}$ |
| $(La_{0.7}Sn_{0.3})_2Mn_2O_7$ | 12.5480 ± 0.04107 | $1.8333 \times 10^{-5} \pm 1.7709 \times 10^{-7}$ |

The value of ρ_0 increases with the increase in Sn concentration. Such a increase in ρ_0 values could be due to the decrease in size of domains or non alignment of spins in grain boundaries such that charge carriers scattering is increased.

4. Conclusion

The compound $La_2Mn_2O_7$ is difficult to synthesize as La and Mn in the presence of oxygen at high temperature will always form the $LaMnO_2$. But in our case we able to index all the peaks using PowderX technique. This indicates that prepared samples $(La_{1-x}Sn_x)_2Mn_2O_7$ ($x = 0.1, 0.2, 0.3$) exist in single phase. The variation in lattice parameters and an increase in unit cell volume have been observed with the increase in Sn concentration. We conclude from our structural analysis that $(La_{1-x}Sn_x)_2Mn_2O_7$ can be formed in single phase form if proper preparation conditions are employed. All the samples exhibit metal insulator transition. In the metallic region ($T < T_c$) resistivity data fits well with the expression: $\rho = \rho_0 + \rho_1 T^n$ with $n = 2$ and 2.5 . This suggests that the electron-electron, electron-phonon, electron-magnon interactions are dominant in this temperature regime ($T < T_c$). The resistivity follows the behavior similar to that of an extrinsic semiconductor above the transition temperature ($T > T_c$). In this temperature range resistivity data fits well with $\rho = \rho T \exp(E_a/k_B T)$. This reveals that conductivity mechanism has the involvement of small polaron hopping.

References

- [1] P. Mandal, S. Das; Phys. Rev. **B 56**, 15073 (1997).
- [2] P. Raychauduri, S. Mukerji, A.K. Nigam, J. John, U.D. Vaisnav, R. Pinto and P. Mandal; J. Appl. Phys. **86**, 5718 (1999).
- [3] C. Mitra, P. Raychaudhuri, J. John, S.K. Dhar, A. K. Nigam and R. Pinto; J. Appl. Phys. **89**, 524 (2001).
- [4] Shahid Husain, R. J. Choudhary, Ravi Kumar, S. I. Patil and J. P. Srivastava; Pramana, **58**, 1045 (2002).
- [5] Ravi Kumar, R. J. Choudhary, S. I. Patil, Shahid Husain, J. P. Srivastava, S. P. Sanyal, S. E. Lofland; J. Appl. Phys., **96**, 7383 (2004).
- [6] J. Gao, S.Y. Dai, T.K. Li, Phys. Phys. Rev. B **67**, 153403 (2003)
- [7] X. X. Guo, S.Y. Dai, Y.L. Zhou, G.Z. Yang, Z.H. Chan, Appl. Phys. Lett. **75**, 3378 (1999)
- [8] X. X. Guo, Z.H. Chen, S.Y. Dai, Y. L. Zhou, R. W. Li, H. W. Zhang, B. G. Shen, H. S. Cheng, J. Appl. Phys. **88**, 4758 (2000)
- [9] C. Zener; Phys. Rev. **82**, 403 (1951).
- [10] A. J. Millis, P. B. Littlewood, B. I. Shraiman; Phys. Rev. Lett. **74**, 5144 (1995).
- [11] J. B. Goodenough in Progress in Solid State Chemistry, edited by H. Reiss (Pergamon, Oxford, 1971) Vol. 5 Ch. 4 pp. 145-150.
- [12] P. Schiffer, A.P. Ramirez, W-Bao, S.W Cheong; Phys. Rev. Lett. **75**, 3336 (1995).

*Corresponding author: s.husain@lycos.com